Estimating the effect of competition on trait evolution using maximum likelihood inference

Jonathan Drury[1]*, Julien Clavel[1], & Hélène Morlon[1]

[1]*Département de Biologie, École Normale Supérieure, 46 rue d'Ulm, 75005 Paris, France*

*Correspondence: drury@biologie.ens.fr, +33 (7) 83 11 43 21

Running head: INTERSPECIFIC COMPETITION & TRAIT EVOLUTION

Abstract

Many classical ecological and evolutionary theoretical frameworks posit that competition between species is an important selective force. For example, in adaptive radiations, resource competition between evolving lineages plays a role in driving phenotypic diversification and exploration of novel ecological space. Nevertheless, current models of trait evolution fit to phylogenies and comparative datasets are not well designed for incorporating the effect of competition. The most advanced models in this direction are diversity-dependent models where evolutionary rates depend on lineage diversity. However, these models still treat changes in traits in one branch as independent of the value of traits on other branches, thus ignoring the effect of species similarity on trait evolution. Here, we consider a model where the evolutionary dynamics of traits involved in interspecific interactions are influenced by species similarity in trait values and where we can specify which lineages are in sympatry. We develop a maximum-likelihood based approach to fit this model to combined phylogenetic and phenotypic data. Using simulations, we demonstrate that the approach accurately estimates the simulated parameter values across a broad range of parameter space. Additionally, we develop tools for specifying the biogeographic context in which trait evolution occurs. In order to compare models, we also apply these biogeographic methods to specify which lineages interact sympatrically for two diversity-dependent models. Finally, we fit these various models to morphological data from a classical adaptive radiation (Greater Antillean *Anolis* lizards). We show that models that account for competition and geography perform better than other models. Given the importance of interspecific interactions, in particular competition, in many ecological and evolutionary processes, this model is an important new tool for using comparative datasets to study phenotypic evolution.

Keywords: interspecific competition, phylogenetic comparative methods, adaptive radiation, trait evolution, *Anolis*, maximum likelihood

Interactions between species can be strong selective forces. Indeed, many classical evolutionary theories assume that interspecific competition has large impacts on fitness. Character displacement theory (Brown and Wilson 1956; Grant 1972; Pfennig and Pfennig 2009), for example, posits that interactions between species, whether in ecological or social contexts, drive adaptive changes in phenotypes. Similarly, adaptive radiation theory has been a popular focus of investigators interested in explaining the rapid evolution of phenotypic disparity (Grant and Grant 2002; Losos 2009; Mahler et al. 2013; Weir and Mursleen 2013), and competitive interactions between species in a diversifying clade are a fundamental component of adaptive radiations (Schluter 2000; Losos and Ricklefs 2009; Grant and Grant 2011).

Additionally, social interactions between species, whether in reproductive (Gröning and Hochkirch 2008; Pfennig and Pfennig 2009) or agonistic (Grether et al. 2009, 2013) contexts, are important drivers of changes in signal traits used in social interactions. Several evolutionary hypotheses predict that geographical overlap with closely related taxa should drive divergence in traits used to distinguish between conspecifics and heterospecifics (Wallace 1889; Fisher 1930; Dobzhansky 1940; Mayr 1963; Gröning and Hochkirch 2008; Ord and Stamps 2009; Ord et al. 2011). Moreover, biologists interested in speciation have often argued that interspecific competitive interactions are important drivers of divergence between lineages that ultimately leads to reproductive isolation. Reinforcement, or selection against hybridization (Dobzhansky

52 1937, 1940), for example, is often thought to be an important phase of speciation (Grant 1999;
53 Coyne and Orr 2004; Rundle and Nosil 2005; Pfennig and Pfennig 2009).

54 Despite the preponderance of classical evolutionary processes that assume that
55 interspecific interactions have important fitness consequences, existing phylogenetic models of
56 trait evolution treat trait evolution within a lineage as independent from traits in other lineages.
57 For example, in the commonly-used Brownian motion and Ornstein-Uhlenbeck models of trait
58 evolution (Cavalli-Sforza & Edwards 1967, Felsenstein 1988), once an ancestor splits into two
59 daughter lineages, the trait values in those daughter lineages do not depend on the trait values of
60 sister taxa. Some investigators have indirectly incorporated the influence of interspecific
61 interactions by fitting models where evolutionary rates at a given time depend on the diversity of
62 lineages at that time (e.g., the "diversity-dependent" models of Mahler et al. 2010, Weir and
63 Mursleen 2013). While these models capture some parts of the interspecific processes of central
64 importance to evolutionary theory, such as the influence of ecological opportunity, they do not
65 explicitly account for trait-driven interactions between lineages, as trait values in one lineage do
66 not vary directly as a function of trait values in other evolving lineages.

67 Recently, Nuismer and Harmon (2015) proposed a model where the evolution of a
68 species' trait depends on other species' traits. In particular, they consider a model, which they
69 refer to as the model of phenotype matching, where the probability that an encounter between
70 two individuals has fitness consequences declines as the phenotypes of the individuals become
71 more dissimilar. The consequence of the encounter on fitness can be either negative if the
72 interaction is competitive, resulting in character divergence (matching competition, e.g. resource
73 competition), or positive if the interaction is mutualistic, resulting in character convergence
74 (matching mutualism, e.g. Müllerian mimicry). Applying Lande's formula (Lande 1976) and

given a number of simplifying assumptions—importantly that all lineages evolve in sympatry—this model yields a simple prediction for the evolution of a population's mean phenotype.

Here, we develop inference tools for fitting the matching competition model (i.e., the phenotype matching model of Nuismer and Harmon incorporating competitive interactions between lineages) to combined phylogenetic and trait data. We begin by showing how to compute likelihoods associated with this model. Next, we use simulations to explore the statistical properties of maximum likelihood estimation of the matching competition model (parameter estimation as well as the power and type I error rates). While the inclusion of interactions between lineages is an important contribution to quantitative models of trait evolution, applying the matching competition model to an entire clade relies on the assumption that all lineages in the clade are sympatric. However, this assumption will be violated in most empirical cases, so we also developed a method for incorporating data on the biogeographical overlap between species for this model and for the linear and exponential diversity-dependent trait models of Weir & Mursleen (2013), wherein the evolutionary rate at a given time in a tree varies as a function of the number of lineages in the reconstructed phylogeny at that time (see also Mahler et al. 2010).

We then fit the model to data from a classical adaptive radiation: Greater Antillean *Anolis* lizards (Harmon et al. 2003; Losos 2009). Many lines of evidence support the hypothesis that resource competition is responsible for generating divergence between species in both habitat use (e.g., Pacala and Roughgarden 1982) and morphology (Schoener 1970; Williams 1972; see review in Losos 1994). Thus, we can make an *a priori* prediction that model comparison will uncover a signature of competition in morphological traits that vary with habitat and resource use. However, in spite of the importance of interspecific competition to adaptive radiation

98 theory, the role of competition in driving adaptive divergence has been historically difficult to
99 measure (Losos 2009) because trait divergence resulting from competition between lineages
100 during their evolutionary history should have the effect of eliminating competition between those
101 lineages at the present. Nevertheless, the signature of such competition may be detectable in the
102 contemporary distribution of trait values and their covariance structure (Hansen and Martins
103 1996; Nuismer and Harmon 2015), and as such, the matching competition model should provide
104 a good fit to morphological data collected on anoles. Given the well-resolved molecular
105 phylogeny (Mahler et al. 2010, 2013) and the relatively simple geographical relationships
106 between species (i.e., species are restricted to single islands, Rabosky and Glor 2010; Mahler and
107 Ingram 2014), the Greater Antillean *Anolis* lizards provide a good test system for exploring the
108 effect of competition on trait evolution using the matching competition model.
109

110 **METHODS**

111 *Likelihood Estimation of the Matching Competition Model*

112 We consider the evolution of a quantitative trait under the matching competition model of
113 Nuismer & Harmon (2015) wherein trait divergence between lineages will be favored by
114 selection. In our version of the model, we remove stabilizing selection to focus on the effect of
115 competition. The evolution of a population's mean phenotype is thus given by (Eq. S38 in
116 Nuismer & Harmon 2015 with $\psi = 0$):
117

118 $$\bar{z}_i^{'} = \bar{z}_i + S(\mu - \bar{z}_i) + \delta \qquad \text{(Eq. 1)}$$

119

where drift is incorporated as a Gaussian variable δ with mean = 0 and variance = σ^2 (the Brownian motion rate parameter) and S measures the strength of interaction (more intense competitive interactions are represented by larger negative values), $\overline{z}_i^{'}$ is the mean trait value for lineage i after a infinitesimally small time step, and μ is the mean trait value for the entire clade at the beginning of that time step. Hence, if a species trait value is greater (respectively smaller) than the trait value average across species in the clade, the species' trait will evolve towards even larger (respectively smaller) trait values.

Like several other models of quantitative trait evolution (Harmon et al. 2010, Weir & Mursleen 2013), the expected distribution of trait values on a given phylogeny under the matching competition model follows a multivariate normal distribution with mean vector made of terms each equal to the character value at the root of the tree and variance-covariance matrix determined by the parameter values and phylogeny. Nuismer & Harmon (2015) provide the system of ordinary differential equations describing the evolution of the variance and covariance terms through time (their Eqs.10b and 10c). These differential equations can be integrated numerically from the root to the tips of phylogenies to compute expected variance-covariance matrices and the associated likelihood values given by the multivariate normal distribution.

Additionally, to relax the assumption that all of the lineages in a clade coexist sympatrically, we included a term to specify which lineages co-occur at any given time-point in the phylogeny, which can be inferred, e.g., by biogeographical reconstruction. The resulting system of ordinary differential equations describing the evolution of the variance and covariance terms through time are:

143 $$\frac{dv_i^2}{dt} = -\left(\frac{2(n_i-1)}{n_i}S\right)v_i^2 + \frac{2S}{n_i}\left(\sum_{\substack{j=1 \\ (j\neq i)}}^{n} \mathbf{A}_{i,j}v_{i,j}\right) + \sigma^2 \quad \text{(Eq. 2a)}$$

144

145 $$\frac{dv_{i,j}}{dt} = -\left(\frac{2(n_i-1)}{n_i}S\right)v_{i,j} + \frac{S}{n_i}\left(\sum_{\substack{k=1 \\ k\neq j}}^{n} \mathbf{A}_{i,k}v_{i,k} + \sum_{\substack{l=1 \\ l\neq i}}^{n} \mathbf{A}_{j,l}v_{j,l}\right) \quad \text{(Eq. 2b)}$$

146

147 where v_i is the variance for each species *i* at time *t* and $v_{i,j}$ is the covariance for each species pair
148 *i,j* at time *t*. Eq. 2b describes the evolution of the covariance at time *t* if species *i* and *j* are in
149 sympatry at time *t* . If they are not, $\frac{dv_{i,j}}{dt} = 0$ such that the covariance between species *i* and *j*
150 remains fixed, The terms σ^2 and *S* are as specified above, $\mathbf{A}_{i,j}$ equals 1 at time *t* if *i* and *j* are
151 sympatric at that time, and 0 otherwise (Fig. 1), and $n_i = \sum_{j=1}^{n} A_{ij}$ is the number of lineages
152 interacting with lineage *i* at time *t* (equal to the number *n* of lineages in the reconstructed
153 phylogeny at time *t* if all species are sympatric). Here, we consider the matrix **A** to be a block
154 diagonal matrix, such that sets of interacting species are non-overlapping, as in the case of *Anolis*
155 lizards (Fig. 1). This implies that if species *i* and *j* are sympatric, then $n_i = n_j$ and $v_{i,j} = v_{j,i}$.
156 Note that when *S* = 0 or *n* = 1 (i.e., when a species is alone), this model reduces to Brownian
157 motion. This model has three free parameters: σ^2, *S* and the ancestral state z_0 at the root. As with
158 other models of trait evolution, the maximum likelihood estimate for the ancestral state is
159 computed through GLS using the estimated variance-covariance matrix (Grafen 1989; Martins
160 and Hansen 1997).

161 We used the ode function in the R package deSolve (Soetaert et al. 2010) to perform the
162 numerical integration of the differential equations using the "lsoda" solver, and the Nelder-Mead
163 algorithm implemented in the optim function to perform the maximum likelihood optimization.

Codes for these analyses are freely available on github (https://github.com/hmorlon/PANDA) and included the R package RPANDA (Morlon 2014).

Incorporating Geography into Diversity-Dependent Models

Using the same geography matrix **A** described above for the matching competition model (Fig. 1), we modified the diversity-dependent linear and exponential models of Weir & Mursleen (2013) to incorporate biological realism into the models, because ecological opportunity is only relevant within rather than between biogeographical regions. The resulting variance-covariance matrices, **V**, of these models have the elements:

$$\mathbf{V}_{ij} = \sum_{m=2}^{M}(\sigma_0^2 + bn_i)(\max(s_{ij} - t_{m-1}, 0) - \max(s_{ij} - t_m, 0)) \qquad \text{(Eq. 3)}$$

for the diversity-dependent linear model, and

$$\mathbf{V}_{ij} = \sum_{m=2}^{M}(\sigma_0^2 \times e^{rn_i})(\max(s_{ij} - t_{m-1}, 0) - \max(s_{ij} - t_m, 0)) \qquad \text{(Eq. 4)}$$

for the diversity-dependent exponential model, where σ_0^2 is the rate parameter at the root of the tree, b and r are the slopes in the linear and exponential models, respectively, s_{ij} is the shared path length of lineages i and j from the root of the phylogeny to their common ancestor, n_i is the number of sympatric lineages (as above) between nodes at times t_{m-1} and t_m (where t_1 is 0, the time at the root, and t_M is the total length of the tree) (Weir & Mursleen 2013). When b or $r = 0$, these models reduce to Brownian motion.

187 *Simulation-based Analysis of Statistical Properties of the Matching Competition Model*

188 To verify that the matching competition model can be reliably fit to empirical data, we
189 simulated trait datasets to estimate its statistical properties (i.e., parameter estimation, power, and
190 type I error rates). For all simulations, we began by first generating 100 pure-birth trees using
191 TreeSim (Stadler 2014). To determine the influence of the number of tips in a tree, we ran
192 simulations on trees of size n = 20, 50, 100, and 150. We then simulated continuous trait datasets
193 by applying the matching competition model recursively from the root to the tip of each tree
194 (Paradis 2011), following Eq. 1. For these simulations, we set σ^2 = 0.05 and systematically
195 varied S (-1.5, -1, -0.5, -0.1, or 0). Finally, we fit the matching competition model to these
196 datasets using the ML optimization described above.

197 To determine the ability of the approach to accurately estimate simulation parameter
198 values, we first compared estimated parameters to the known parameters used to simulate
199 datasets under the matching competition model (S and σ^2). We also quantified the robustness of
200 these estimates in the presence of extinction by estimating parameters for datasets simulated on
201 birth-death trees; in addition, we compared the robustness of the matching competition model to
202 extinction to that of the diversity-dependent models. These two latter sets of analyses are
203 described in detail in the Supplementary Appendix 1.

204 To assess the power of the matching competition model, we compared the fit of this
205 model to other commonly used trait models on the same data (i.e. data simulated under the
206 matching competition model). Specifically, we compared the matching competition model to (1)
207 Brownian motion (BM), (2) Ornstein-Uhlenbeck/single-stationary peak model (OU, Hansen &
208 Martin 1996), (3) exponential time-dependent (TD_{exp}, i.e., the early burst model, or the ACDC
209 model with the rate parameter set to be negative, Blomberg et al. 2003; Harmon et al. 2010), (4)

210 linear time-dependent evolutionary rate (TD_{lin}, Weir and Mursleen 2012), (5) linear rate
211 diversity-dependent (DD_{lin}, Mahler et al. 2010; Weir and Mursleen 2013), and (6) exponential
212 rate diversity-dependent (DD_{exp}, Weir and Mursleen 2013). These models were fitted using
213 geiger (Harmon et al. 2008) when available there (BM, OU, TD_{exp}, TD_{lin}), or using our own
214 codes, available in RPANDA (Morlon 2014) when they were not available in geiger (DD_{lin},
215 DD_{exp}). Support for each model was determined using Akaike weights (Burnham and Anderson
216 2002).

217 We assessed the type I error rate of the matching competition model by calculating the fit
218 of this model to datasets simulated under the same trait models mentioned above. For BM and
219 OU models, we generated datasets from simulations using parameter values from the appendix of
220 Harmon et al. 2010 scaled to a tree of length 400 (BM, $\sigma^2 = 0.03$; OU, $\sigma^2 = 0.3$, $\alpha = 0.06$). For
221 both the linear and exponential versions of the time- and diversity-dependent models, we
222 simulated datasets with starting rates of $\sigma^2 = 0.6$ and ending rates of $\sigma^2 = 0.01$, declining with a
223 slope determined by the model and tree (e.g., for time-dependent models, the slope is a function
224 of the total height of the tree; for the TD_{exp} model, these parameters result in a total of 5.9 half-
225 lives elapsing from the root to the tip of the tree, Slater and Pennell 2014). These simulations
226 were performed using our own codes, available in RPANDA (Morlon 2014). As above, we
227 calculated the Akaike weights for all models for each simulated dataset.

228

229 *Fitting the Matching Competition Model of Trait Evolution to Caribbean* Anolis *Lizards*

230 To determine whether the matching competition model is favored over models that ignore
231 interspecific interactions in an empirical system where competition is known to have influenced
232 character evolution, we fit the matching competition model to a morphological dataset on adult

233 males of 100 species of Greater Antillean *Anolis* lizards and the time calibrated, maximum clade
234 credibility tree calculated from a Bayesian sample of molecular phylogenies (Mahler et al. 2010,
235 2013; Mahler and Ingram 2014). We included the first four size-corrected phylogenetic principal
236 components from a set of 11 morphological measurements, collectively accounting for 93% of
237 the cumulative variance explained (see details in Mahler et al. 2013). Together, the shape axes
238 quantified by these principal components describe the morphological variation associated with
239 differences between classical ecomorphs in Caribbean anoles (Williams 1972). In addition to the
240 matching competition model, we fit the six previously mentioned models (BM, OU, TD_{exp}, TD_{lin},
241 DD_{exp}, and DD_{lin}) to the *Anolis* dataset.
242 For the matching competition model and diversity-dependent models, to determine the
243 influence of designating clades as sympatric and allopatric, we fit the model for each trait using
244 two sets of geography matrices (i.e., **A** in Eq. 1b, 2, & 3, see Fig. 1): one where all lineages were
245 set as sympatric, and another following the biogeographical reconstruction presented in Fig 18.3
246 of Mahler and Ingram (2014). To simplify the ML optimization, we restricted *S* to take negative
247 values while fitting the matching competition model including the biogeographical relationships
248 among taxa.
249
250 **RESULTS**
251 *Statistical Properties of the Matching Competition Model*
252 Across a range of *S* values, maximum likelihood optimization returns reliable estimates
253 of parameter values (Fig. 2). As the number of tips increases, so does the reliability of maximum
254 likelihood parameter values (Fig. 2). Parameter estimates remain reliable in the presence of
255 extinction, unless the extinction fraction is very large (Supplementary Appendix 1). When

256 datasets are simulated under the matching competition model, model selection generally picks
257 the matching competition model as the best model (Figs. 3, S1); the strength of this
258 discrimination depends on both the *S* value used to simulate the data and the size of the tree
259 (Figs. 3, S1).

260 We found that the matching competition model behaves similarly to a model of declining
261 evolutionary rates through time, as the rate parameter values of the TD_{exp} model estimated on
262 data generated under the matching competition model became increasingly negative under
263 increasing levels of competition (Fig. S2). The dynamics of this declining rate were better
264 described by an exponential decline in rates than by a linear one (Table S1).

265 Simulating datasets under BM, OU, DD_{exp}, and DD_{lin} generating models, we found that
266 there is a reasonably low type I error rate for the matching competition model (Fig. 4a,b,e,f).
267 When character data were simulated under a TD_{lin} model of evolution, the matching competition
268 and/or the diversity-dependent models tended to have lower AICc values than the TD_{lin} model,
269 especially among smaller trees (Figure 4d). For data generated under a TD_{exp} model, model
270 selection always favored the matching competition model over the TD_{exp} model (Fig. 4c).

271

272 *Competition in Greater Antillean* Anolis *Lizards*

273 For the first four phylogenetic principal components describing variation in *Anolis*
274 morphology, we found that models that incorporate species interactions fit the data better than
275 models that ignore them (Table 1). PC1 and PC3, which describe variation in hindlimb/hindtoe
276 and forelimb/foretoe length (Mahler et al. 2013), respectively, are fit best by the matching
277 competition model. PC2 and PC4, which describe variation in body size (snout vent length) and
278 lamellae number, respectively, are fit best by the exponential diversity-dependent model.

279 Additionally, in every case, models that incorporated the geographic relationships among species
280 in the tree outperformed models that assumed that lineages interact in sympatry at the clade level
281 (Table 1).
282
283 **DISCUSSION**
284 The inference methods we present here represent an important new addition to the
285 comparative trait analysis toolkit. Whereas previous models had not accounted for the influence
286 of trait values in other lineages on character evolution, the matching competition model takes
287 these into account. Furthermore, extending both the matching competition model and two
288 diversity-dependent trait evolution models to incorporate geographic networks of sympatry
289 further extends the utility and biological realism of these models.
290 We found that the matching competition property has increasing power and accuracy of
291 parameter estimation with increasing tree sizes and competition strength. We also found that, for
292 most of the generating models we tested (but see below), the matching competition model is not
293 erroneously favored using model selection (i.e., there is a reasonably low type-I error rate). As
294 with all other models, the statistical properties of the matching competition model will depend on
295 the size and shape of a particular phylogeny as well as specific model parameter values. Future
296 investigators can employ other approaches, such as phylogenetic Monte Carlo and posterior
297 predictive simulations directly on their empirical trees (Boettiger et al. 2012, Slater & Pennell
298 2014), to assess the confidence they can have in their results
299 We found that data generated under time-dependent models were often fit better by
300 models that incorporate interspecific interactions (i.e., density-dependent and matching
301 competition models) (Fig. 4c,d). This was especially true for the TD_{exp} model, often referred to

302 as the early-burst model—the matching competition model nearly always fit data generated
303 under the TD_{exp} model better than the TD_{exp} model (Fig. 4c). We do not view this as a major
304 limitation of the model for two reasons. First, the TD_{exp} model is known to be statistically
305 difficult to estimate on neontological data alone (Harmon et al. 2010; Slater et al. 2012; Slater
306 and Pennell 2014). Accordingly, since the matching competition model also describes declining
307 evolutionary rates from the root to the tip of the tree (Fig. S2, Table S1), it is perhaps not
308 surprising that the matching competition model fits data generated under the TD_{exp} model well.
309 Secondly, and more importantly, time-dependent models are not process-based models, but
310 rather incorporate time since the root of a tree as a proxy for ecological opportunity or available
311 niche space (Harmon et al. 2010; Mahler et al. 2010; Slater 2015). The matching competition and
312 density-dependent models explicitly account for the interspecific competitive interactions that
313 time-dependent models purport to model, thus we argue that these process-based models are
314 more biologically meaningful than time-dependent models (Moen and Morlon 2014).
315 Because the matching competition model depends on the mean trait values in an evolving
316 clade, maximum likelihood estimation is robust to extinction, whereas the diversity-dependent
317 models are less so (Appendix S1, Figs. S3-S6). Nevertheless, given the failure of maximum
318 likelihood to recover accurate parameter estimations at high levels of extinction (μ: $\lambda \geq 0.6$), we
319 suggest that these models should not be used in clades where the extinction rate is known to be
320 particularly high. In such cases, it would be preferable to adapt the inference framework
321 presented here to include data from fossil lineages (Slater et al. 2012), which could be easily
322 done by integrating the ordinary differential equations described in Eq. 2a and 2b on non-
323 ultrametric trees.

For all of the traits we analyzed, we found that models incorporating both the influence of other lineages and the specific geographical relationships among lineages were the most strongly supported models (though less strikingly for PC3 and PC4). The matching competition model is favored in the PCs describing variation in relative limb size. Previous research demonstrates that limb morphology explains between-ecomorph variation in locomotive capabilities and perch characteristics (Losos 1990, 2009; Irschick et al. 1997), and our results suggest that the evolutionary dynamics of these traits have been influenced by the evolution of limb morphology in other sympatric lineages. These results support the assumption that interspecific interactions resulting from similarity in trait values are important components of adaptive radiations (Losos 1994, Schluter 2000), a prediction that has been historically difficult to test (Losos 2009, but see Mahler et al. 2010). In combination with previous research demonstrating a set of convergent adaptive peaks to which lineages are attracted (Mahler et al. 2013), our results suggest that competition likely played an important role in driving lineages toward these distinct peaks.

We imagine that the matching competition model and biogeographical implementations of diversity-dependent models will play a substantial role in comparative studies of interspecific competition. There are many possible extensions of the tools developed in this paper. In the current implementation of interspecific geographic overlap, the matrices of sympatry/allopatry are assumed to be block diagonal matrices. In the future, the model can be extended to more complex geography matrices that are more realistic for mainland taxa (e.g., using ancestral biogeographical reconstruction, Ronquist and Sanmartín 2011; Landis et al. 2013), and can also specify degrees of sympatric overlap (i.e., syntopy). Additionally, although the current version of the model is rather computationally expensive with larger trees (with 100 or more tips), future work to speed up the calculation of the variance-covariance matrix under the matching

347 competition model would allow the inclusion of uncertainty in biogeographical reconstruction
348 (e.g., from samples of stochastic maps). The current form of the model assumes that the degree
349 of competition is equal for all interacting lineages. Future modifications of the model, such as
350 applications of stepwise AICc algorithms (Alfaro et al. 2009; Thomas and Freckleton 2012;
351 Mahler et al. 2013) or reversible-jump Markov Chain Monte Carlo (Pagel and Meade 2006;
352 Eastman et al. 2011; Rabosky 2014; Uyeda and Harmon 2014), may be useful to either identify
353 more intensely competing lineages or test specific hypotheses about the strength of competition
354 between specific taxa. Improvements could also be made on the formulation itself of the
355 evolution of a species' trait as a response to the phenotypic landscape in which the species
356 occurs. The current formulation (Eq. 1) corresponds to a scenario in which the rate of phenotypic
357 evolution on a lineage gets higher as the lineage deviates from the mean phenotype, although
358 character displacement theory, for example, posits that selection for divergence should be the
359 strongest when species are most ecologically similar (Brown & Wilson 1956). Finally, a great
360 array of extensions will come from modeling species interactions not only within clades, but also
361 among interacting clades, as in the case of coevolution in bipartite mutualistic or antagonistic
362 networks, such as plant-pollinator or plant-herbivore systems (Bartosek et al. 2012).
363 In addition to uncovering a signature of competitive interactions in traits used in
364 exploitative competition for resources (e.g., trait-axes along which adaptive radiations proceed,
365 Schluter 2000), the tools presented here can be used to test several hypotheses that have
366 historically been difficult to test using phylogenetic comparative methods. For example, various
367 hypotheses about the dynamics of traits involved in social interactions that posit that interspecific
368 interactions have played an important role in shaping contemporary trait values (e.g., Pfennig
369 and Pfennig 2012; Grether et al. 2013) are beginning to be tested at comparative scales (Seddon

370 et al. 2013; Tobias et al. 2013; Martin et al. 2015). However, the tools available for such analyses
371 have been limited (e.g., sister-taxa comparisons) relative to those available to test
372 macroevolutionary hypotheses about within-taxa processes. By comparing the fits of the
373 matching competition model with other models that do not include competitive interactions
374 between lineages, biologists can directly test hypotheses that make predictions about the role of
375 interspecific interactions in driving trait evolution.
376

377 **Acknowledgements**

378 We thank M. Manceau for his help troubleshooting the inference approach, J. Weir for
379 providing R code for diversity-dependent models, and E. Lewitus and O. Missa for helpful
380 comments on the manuscript. This research was funded by the Agence Nationale de la Recherche
381 (grant CHEX-ECOEVOBIO); and the European Research Council (grant 616419-PANDA to
382 HM).
383
384

385 **References**

386 Alfaro M.E., Santini F., Brock C., Alamillo H., Dornburg A., Rabosky D.L., Carnevale G.,
387 Harmon L.J. 2009. Nine exceptional radiations plus high turnover explain species diversity
388 in jawed vertebrates. Proc. Natl. Acad. Sci. 106:13410–13414.

389 Bartosek K., Pienaar J., Mostad P., Andersson S., Hansen T.F. 2012. A phylogenetic
390 comparative method for studying multivariate adaptation. J. of Theor. Biol. 314:204-215.

391 Blomberg S.P., Garland T., Ives A.R. 2003. Testing for phylogenetic signal in comparative data:
392 behavioral traits are more labile. Evolution. 57:717–745.

393 Boettiger C., Coop G., Ralph P. 2012. Is Your Phylogeny Informative ? Measuring the Power of
394 Comparative Methods. Evolution 66:2240–2251.

395 Brown W.L., Wilson E.O. 1956. Character Displacement. Syst. Zool. 5:49-62.

396 Burnham K.P., Anderson D.R. 2002. Model selection and multimodel inference: a practical
397 information-theoretic approach. New York, NY: Springer.

398 Cavalli-Sforza, L.L., Edwards, A.W.F. 1967. Phylogenetic analysis: Models and estimation
399 procedures. Amer. J. of Hum. Gen. 19:233-257.

400 Coyne J.A., Orr H.A. 2004. Speciation. Sunderland, MA: Sinauer Associates.

401 Dobzhansky T. 1937. Genetics and the Origin of Species. New York, NY: Columbia University
402 Press.

Dobzhansky T. 1940. Speciation as a stage in evolutionary divergence. Am. Nat. 74:312–321.

Eastman J.M., Alfaro M.E., Joyce P., Hipp A.L., Harmon L.J. 2011. A novel comparative method for identifying shifts in the rate of character evolution on trees. Evolution 65:3578–3589.

Felsenstein, J. 1988. Phylogenies and quantitative characters. Ann. Rev. of Ecol., Evol., & Systematics. 19:445-471.

Fisher R.A. 1930. The Genetical Theory of Natural Selection. Oxford, UK.: Oxford University Press.

Grafen A. 1989. The phylogenetic regression. Philos. Trans. R. Soc. Lond. B. Biol. Sci. 326:119–157.

Grant P.R., Grant B.R. 2002. Adaptive radiation of Darwin's finches: Recent data help explain how this famous group of Galápagos birds evolved, although gaps in our understanding remain. Am. Sci. 90:130–139.

Grant P.R., Grant B.R. 2011. How and Why Species Multiply: the Radiation of Darwin's Finches. Princeton, NJ: Princeton University Press.

Grant P.R. 1972. Convergent and divergent character displacement. Biol. J. Linn. Soc. 4:39–68.

Grant P.R. 1999. Ecology and Evolution of Darwin's finches. Princeton, NJ: Princeton University Press.

421 Grether G.F., Anderson C.N., Drury J.P., Kirschel A.N.G., Losin N., Okamoto K., Peiman K.S.
422 2013. The evolutionary consequences of interspecific aggression. Ann. N. Y. Acad. Sci.
423 1289:48–68.

424 Grether G.F., Losin N., Anderson C.N., Okamoto K. 2009. The role of interspecific interference
425 competition in character displacement and the evolution of competitor recognition. Biol.
426 Rev. 84:617–635.

427 Gröning J., Hochkirch A. 2008. Reproductive interference between animal species. Q. Rev. Biol.
428 83:257–282.

429 Hansen T.F., Martins E.P. 1996. Translating between microevolutionary process and
430 macroevolutionary patterns: The correlation structure of interspecific data. Evolution
431 50:1404–1417.

432 Harmon L.J., Losos J.B., Jonathan Davies T., Gillespie R.G., Gittleman J.L., Bryan Jennings W.,
433 Kozak K.H., McPeek M.A., Moreno-Roark F., Near T.J., Purvis A., Ricklefs R.E., Schluter
434 D., Schulte J.A., Seehausen O., Sidlauskas B.L., Torres-Carvajal O., Weir J.T., Mooers
435 A.T. 2010. Early bursts of body size and shape evolution are rare in comparative data.
436 Evolution 64:2385–2396.

437 Harmon L.J., Schulte J.A., Larson A., Losos J.B. 2003. Tempo and mode of evolutionary
438 radiation in iguanian lizards. Science 301:961–964.

439 Harmon L.J., Weir J.T., Brock C.D., Glor R.E., Challenger W. 2008. GEIGER: investigating
440 evolutionary radiations. Bioinformatics. 24:129–131.

441 Irschick D.J., Vitt L.J., Zani P.A., Losos J.B. 1997. A comparison of evolutionary radiations in
442 mainland and Caribbean Anolis lizards. Ecology. 78:2191–2203.

443 Landis M.J., Matzke N.J., Moore B.R., Huelsenbeck J.P. 2013. Bayesian analysis of
444 biogeography when the number of areas is large. Syst. Biol. 62:789–804.

445 Losos J.B., Ricklefs R.E. 2009. Adaptation and diversification on islands. Nature. 457:830–836.

446 Losos J.B. 1990. The evolution of form and function: morphology and locomotor performance in
447 West Indian Anolis lizards. 44:1189–1203.

448 Losos J.B. 1994. Integrative Approaches to Evolutionary Ecology: Anolis Lizards as Model
449 Systems. Annu. Rev. Ecol. Syst. 25:467–493.

450 Losos J.B. 2009. Lizards in an Evolutionary Tree: Ecology and Adaptive Radiation of Anoles.
451 Los Angeles, CA: University of California Press.

452 Mahler D.L., Ingram T., Revell L.J., Losos J.B. 2013. Exceptional convergence on the
453 macroevolutionary landscape in island lizard radiations. Science 341:292–5.

454 Mahler D.L., Ingram T. 2014. Phylogenetic Comparative Methods for Studying Clade-Wide
455 Convergence. In: Garamszegi L., editor. Modern Phylogenetic Comparative Methods and
456 Their Application in Evolutionary Biology. New York, NY: Springer. p. 425–450.

457 Mahler D.L., Revell L.J., Glor R.E., Losos J.B. 2010. Ecological opportunity and the rate of
458 morphological evolution in the diversification of greater Antillean anoles. Evolution
459 64:2731–2745.

460 Martin P.R., Montgomerie R., Lougheed S.C. 2015. Color patterns of closely related bird species
461 are more divergent at intermediate levels of breeding-range sympatry. Am. Nat. 185:443–
462 451.

463 Martins E.P., Hansen T.F. 1997. Phylogenies and the comparative method: a general approach to
464 incorporating phylogenetic information into the analysis of interspecific data. Am. Nat.
465 149:646–667.

466 Mayr E. 1963. Animal Species and Evolution. Cambridge, MA: Harvard University Press.

467 Moen D., Morlon H. 2014. Why does diversification slow down? Trends Ecol. Evol. 29:190–
468 197.

469 Morlon H. 2014. RPANDA: Phylogenetic ANalyses of DiversificAtion. R package version 1.0.
470 https://github.com/hmorlon/PANDA

471 Nuismer S.L., Harmon L.J. 2015. Predicting rates of interspecific interaction from phylogenetic
472 trees. Ecol. Lett. 18:17–27.

473 Ord T.J., King L., Young A.R. 2011. Contrasting theory with the empirical data of species
474 recognition. Evolution 65:2572–2591.

475 Ord T.J., Stamps J.A. 2009. Species identity cues in animal communication. Am. Nat. 174:585–
476 593.

477 Pacala S., Roughgarden J. 1982. Resource partitioning and interspecific competition in two two-
478 species insular Anolis lizard communities. Science 217:444–446.

479 Pagel M., Meade A. 2006. Bayesian analysis of correlated evolution of discrete characters by
480 reversible-jump Markov chain Monte Carlo. Am. Nat. 167:808–825.

481 Paradis E. 2011. Analysis of Phylogenetics and Evolution with R. New York, NY: Springer.

482 Pfennig D.W., Pfennig K.S. 2012. Evolution's Wedge: Competition and the Origins of Diversity.
483 Los Angeles, CA: Univ of California Press.

484 Pfennig K.S., Pfennig D.W. 2009. Character displacement: ecological and reproductive
485 responses to a common evolutionary problem. Q. Rev. Biol. 84:253–276.

486 Rabosky D.L., Glor R.E. 2010. Equilibrium speciation dynamics in a model adaptive radiation of
487 island lizards. Proc. Natl. Acad. Sci. U. S. A. 107:22178–22183.

488 Rabosky D.L. 2014. Automatic detection of key innovations, rate shifts, and diversity-
489 dependence on phylogenetic trees. PLoS One. 9:e89543.

490 Ronquist F., Sanmartín I. 2011. Phylogenetic methods in biogeography. Annu. Rev. Ecol. Evol.
491 Syst. 42:441–464.

492 Rundle H.D., Nosil P. 2005. Ecological speciation. Ecol. Lett. 8:336–352.

493 Schluter D. 2000. The Ecology of Adaptive Radiation. Oxford, UK: Oxford University Press.

494 Schoener T.W. 1970. Size Patterns in West Indian Anolis Lizards. II. Correlations with the Sizes
495 of Particular Sympatric Species-Displacement and Convergence. Am. Nat. 104:155–174.

496 Seddon N., Botero C.A., Tobias J.A., Dunn P.O., Macgregor H.E., Rubenstein D.R., Uy J.A.,
497 Weir J.T., Whittingham L.A., Safran R.J. 2013. Sexual selection accelerates signal
498 evolution during speciation in birds. Proc. R. Soc. B Biol. Sci. 280:20131065.

499 Slater G.J., Harmon L.J., Alfaro M.E. 2012. Integrating fossils with molecular phylogenies
500 improves inference of trait evolution. 66:3931–3944.

501 Slater G.J., Pennell M.W. 2014. Robust regression and posterior predictive simulation increase
502 power to detect early bursts of trait evolution. Syst. Biol. 63:293–308.

503 Soetaert K., Petzoldt T., Setzer R.W. 2010. Solving Differential Equations in R: Package
504 deSolve. J. Stat. Softw. 33:1–25.

505 Stadler T. 2014. TreeSim: Simulating trees under the birth-death model. R package version 2.1.
506 http://CRAN.R-project.org/package=TreeSim.

507 Thomas G.H., Freckleton R.P. 2012. MOTMOT: models of trait macroevolution on trees.
508 Methods Ecol. Evol. 3:145–151.

509 Tobias J.A., Cornwallis C.K., Derryberry E.P., Claramunt S., Brumfield R.T., Seddon N. 2013.
510 Species coexistence and the dynamics of phenotypic evolution in adaptive radiation. Nature.
511 506:359–363.

512 Uyeda J.C., Harmon L.J. 2014. A novel Bayesian method for inferring and interpreting the
513 dynamics of adaptive landscapes from phylogenetic comparative data. Syst. Biol. 63:902–
514 918.

515 Wallace A.R. 1889. Darwinism. 2007 facsimile, Cosimo, Inc.

516 Weir J.T., Mursleen S. 2013. Diversity-dependent cladogenesis and trait evolution in the
517 adaptive radiation of the auks (Aves: Alcidae). Evolution 67:403–416.

518 Williams E.E. 1972. The Origin of Faunas. Evolution of Lizard Congeners in a Complex Island
519 Fauna: A Trial Analysis. Evol. Biol. 6:47–89.

520

521

522 **Table & Figure legends**

523 **Table 1.** Comparison of model fits for the first four phylogenetic principal components of a
524 morphological dataset of Greater Antillean anoles. Models run incorporating geography matrices
525 are indicated by "+ GEO", and models with the lowest AICc for each trait are shaded and written
526 in bold text. Parameter values presented follow the nomenclature of Eqs. 2-4 in the main text,
527 and *k* represents the number of parameters estimated for each model. Note that TD_{exp} is the
528 ACDC model (or the early-burst model when $r < 0$). OU model weights were excluded because
529 α was estimated to be 0 for each trait, and thus the OU model was equivalent to BM.
530

531 *Figure 1.* Illustration of geography matrices (defined between each node) delineating which
532 lineages interact in sympatry in an imagined phylogeny. These matrices were used to identify
533 potentially interacting lineages for the matching competition and both diversity-dependent
534 models of character evolution (see Eqs. 2-4 in the main text). *Anolis* outline courtesy of Sarah
535 Werning, licensed under Creative Commons (http://creativecommons.org/licenses/by/3.0/).
536

537 *Figure 2*. Parameter estimation under the matching competition model. As tree size increases
538 and/or the magnitude of competition increases (i.e., the *S* parameter in the matching competition
539 model becomes more negative), so does the accuracy of ML parameter estimates of (A) *S* (n =
540 100 for each tree size and *S* value combination; red horizontal lines indicate the simulated *S*
541 value) and (B) the accuracy of ML parameter estimates of σ^2 (n = 500 for each tree size; red
542 horizontal lines indicate the simulated σ^2 value). The numbers below the violin plots in (B) show
543 the number of outliers removed for plotting.
544

Figure 3. The statistical power of the matching competition increases with tree size and with increasing levels of competition (i.e., increasingly negative *S* values).

Figure 4. Type-I error simulation results for the matching competition model. When the generating model is either (A) BM, (B) OU, (E) DD_{exp} (for larger trees) or (F) DD_{lin}, the generating model is largely favored by model selection. However, both (C) TD_{exp} and (D) TD_{lin} (for smaller trees) are erroneously rejected as the generating model.

Table 1.

Trait	Model	k	σ^2	b	r	S	ln(Ł)	ΔAICc	Akaike weights
pPC1	BM	2	0.0033	—	—	—	-13.68	22.40	<0.01
	OU	3	0.0033	—	—	—	-13.68	24.52	—
	TDexp	3	0.0324	—	-0.068	—	-5.20	7.55	0.02
	TDlinear	3	0.0113	-0.019	—	—	-4.88	6.92	0.03
	LDexp	3	0.0184	—	-0.028	—	-4.37	5.90	0.04
	LDexp + GEO	3	0.0086	—	-0.043	—	-7.28	11.72	<0.01
	LDlin	3	0.0089	-0.00008	—	—	-4.89	6.94	0.02
	LDlin + GEO	3	0.0042	-0.000042	—	—	-10.34	17.84	<0.01
	MC_{sym}	3	0.0010	—	—	-0.037	-3.67	4.50	0.08
	MC + GEO	**3**	**0.0010**	**—**	**—**	**-0.037**	**-1.42**	**0**	**0.80**
pPC2	BM	2	0.0027	—	—	—	-4.69	8.55	0.01
	OU	3	0.0027	—	—	—	-4.69	10.67	—
	TDexp	3	0.0046	—	-0.014	—	-4.30	9.89	<0.01
	TDlinear	3	0.0047	-0.011	—	—	-4.23	9.75	<0.01
	LDexp	3	0.0041	—	-0.006	—	-4.27	9.84	<0.01
	LDexp + GEO	**3**	**0.0067**	**—**	**-0.039**	**—**	**0.65**	**0**	**0.84**
	LDlin	3	0.0041	-0.00002	—	—	-4.21	9.72	<0.01
	LDlin + GEO	3	0.0035	-0.000035	—	—	-1.57	4.44	0.09
	MC_{sym}	3	0.0021	—	—	-9.9e-3	-3.95	9.19	<0.01
	MC + GEO	3	0.0019	—	—	-0.014	-2.90	7.10	0.02
pPC3	BM	2	0.0010	—	—	—	45.57	1.4	0.11
	OU	3	0.0010	—	—	—	45.57	3.5	—
	TDexp	3	0.0020	—	-0.019	—	46.30	2.06	0.08
	TDlinear	3	0.0019	-0.013	—	—	46.41	1.85	0.09
	LDexp	3	0.0017	—	-0.008	—	46.40	1.86	0.09
	LDexp + GEO	3	0.0015	—	-0.017	—	46.67	1.33	0.11
	LDlin	3	0.0017	-0.000009	—	—	46.46	1.74	0.09
	LDlin + GEO	3	0.0013	-0.000014	—	—	46.58	1.5	0.10
	MC_{sym}	3	0.0007	—	—	-0.012	46.75	1.17	0.12
	MC + GEO	**3**	**0.0007**	**—**	**—**	**-0.015**	**47.33**	**0**	**0.22**
pPC4	BM	2	0.0006	—	—	—	69.07	1.96	0.07
	OU	3	0.0006	—	—	—	69.07	4.09	—
	TDexp	3	0.0015	—	-0.015	—	70.55	1.12	0.10
	TDlinear	3	0.0012	-0.011	—	—	70.45	1.32	0.09
	LDexp	3	0.0012	—	-0.0061	—	70.52	1.18	0.10
	LDexp + GEO	**3**	**0.0010**	**—**	**-0.019**	**—**	**71.11**	**0**	**0.17**
	LDlin	3	0.0011	-0.00002	—	—	70.39	1.45	0.08
	LDlin + GEO	3	0.0008	-0.000035	—	—	70.66	0.92	0.11
	MC	3	0.0004	—	—	-0.015	71.1	0.02	0.17
	MC + GEO	3	0.0004	—	—	-0.013	70.6	1.03	0.10

Figure 1.

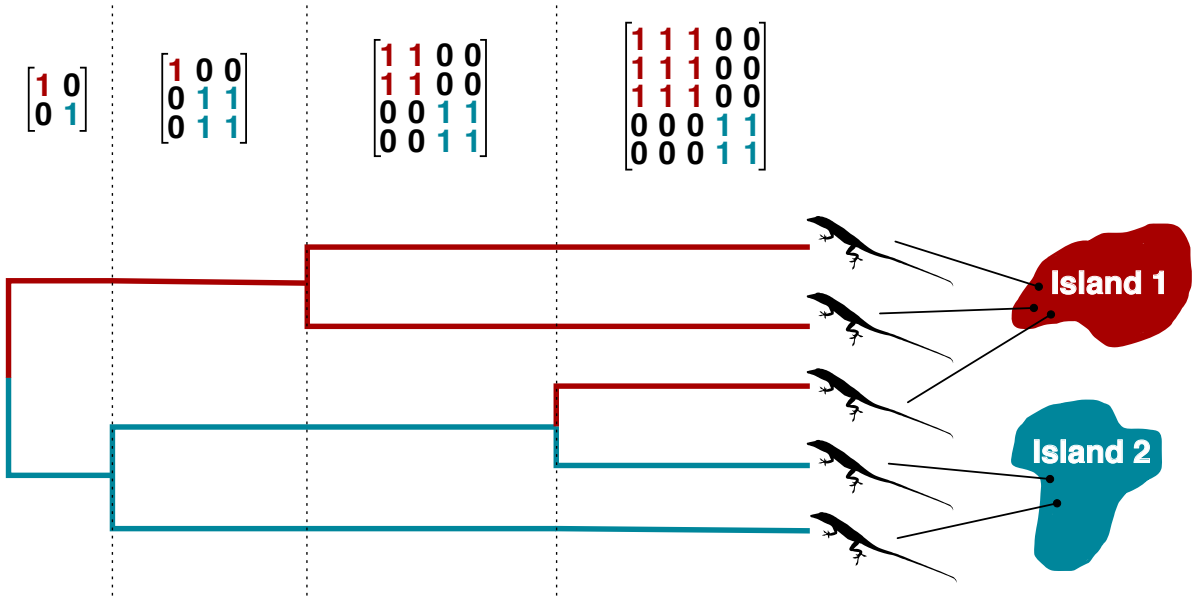

562 Figure 2.

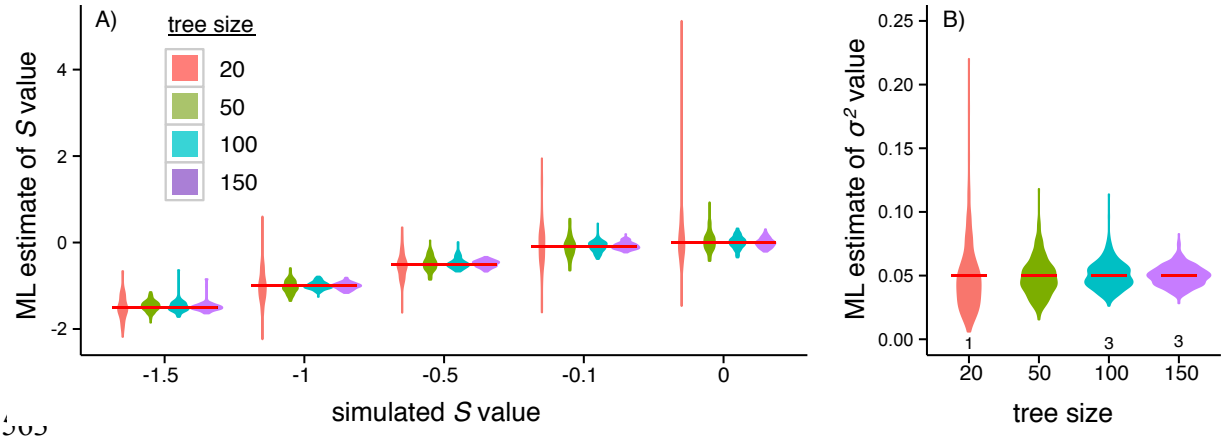

563
564

Figure 3

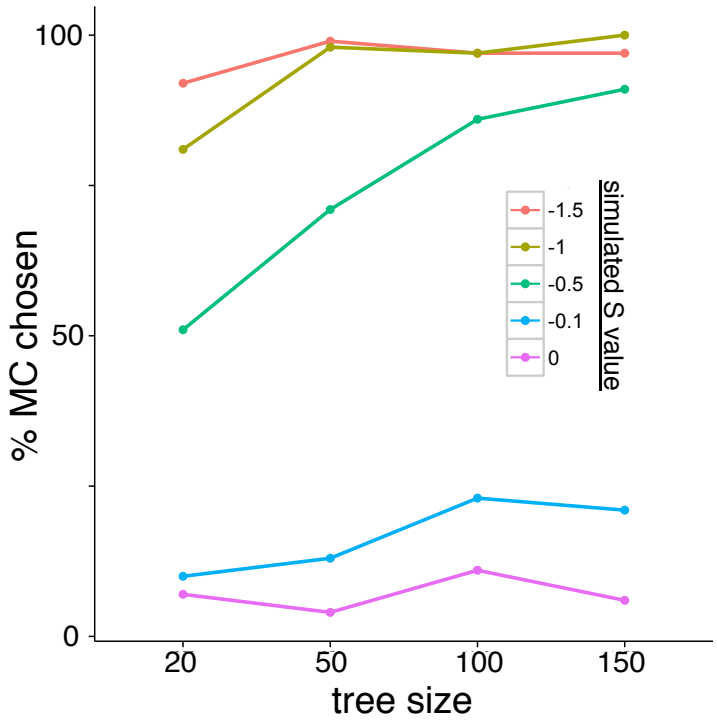
100
50
0
% MC chosen
20
50
100
150
tree size
-1.5
-1
-0.5
-0.1
0
simulated S value

Figure 4.

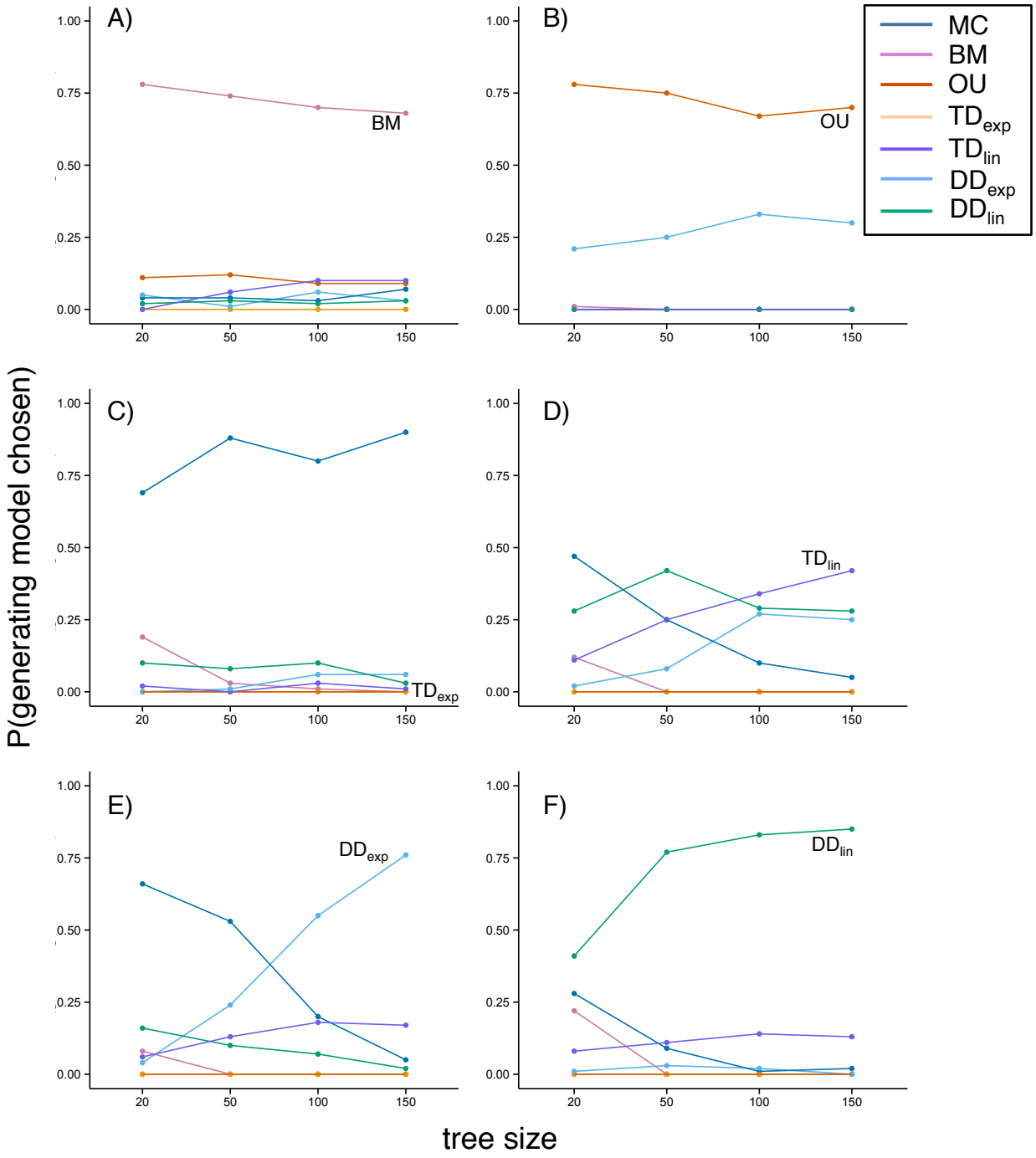
A)
B)
C)
D)
E)
F)
BM
OU
TDexp
TDlin
DDexp
DDlin
MC
BM
OU
TDexp
TDlin
DDexp
DDlin
P(generating model chosen)
tree size
1.00
0.75
0.50
0.25
0.00
20
50
100
150

Supplementary Material

Appendix S1

Table S1

Figure S1-S6

586 *Supplementary Appendix 1:* **Estimating the effect of extinction on parameter estimation for**
587 **the matching competition and density-dependent models.**
588
589 Given that the matching competition and diversity-dependent models take into account
590 the number of interacting lineages, extinction may affect our ability to recover true parameter
591 values. To estimate the impact of extinction, we simulated 100 trees with 100 extant species,
592 varying the extinction fraction (μ: λ = 0.2, 0.4, 0.6, and 0.8). As above, we recursively simulated
593 traits using the matching competition model with σ^2 = 0.05 and S = -1.5, -1, -0.5, -0.1, or 0, and
594 the linear and exponential diversity-dependent models with starting rates of σ^2 = 0.6 and ending
595 rates of σ^2 = 0.01. We then estimated the maximum likelihood parameter estimates for the
596 generating models by fitting the models to the trait values for extant species and the tree with
597 extinct lineages removed. In the case of the matching competition model, because many
598 simulated birth-death trees with high extinction rates have substantially older root ages, the
599 simulated trait datasets for some trees had very large variances. For these biologically unrealistic
600 trait datasets (i.e., variance in trait values $\geq 1\text{x}10^8$), ML does not yield reliable parameter
601 estimates, so we removed them from further analyses (the sample size of included simulations is
602 reported in Fig. S3, S4).
603 Parameter estimates are quite robust to extinction under the matching competition model
604 (Fig. S3, S4), and much more so than under both diversity-dependent models (Fig. S5,S6). Under
605 the matching competition model, the maximum likelihood optimization returns reliable estimates
606 of S and σ^2 values used to simulate datasets on trees with extinct lineages (Fig. S3, S4), although
607 the estimates become much less reliable with larger extinction fractions, likely because
608 simulations under the matching competition model were unbounded, resulting in trait datasets

with biologically unrealistic variances. Under both diversity-dependent models, the magnitude of both the slope and σ^2 parameter values are increasingly underestimated with increasing extinction fractions (Fig. S5, S6).

614 **Table S1.** Data generated under the matching competition model are better fit by the TD_{exp}

615 model than by the TD_{lin} model. ΔAICc [90% CI] presented for the matching competition (MC)

616 and time dependent models.

617

tips	*S* value	MC	TD_{exp}	TD_{lin}
20	-1.5	0 [0, 0.68]	6.04 [3.20, 10.53]	12.17 [1.27, 67.92]
	-1	0 [0, 2.17]	3.96 [1.87, 7.47]	4.18 [0.78, 25.03]
	-0.5	0 [0, 2.76]	2.74 [1.70, 4.06]	2.42 [0.97, 6.36]
	-0.1	2.37 [0, 2.79]	2.79 [1.83, 5.04]	2.1 [0.85, 3.11]
	0	2.47 [0, 2.98]	2.79 [2.17, 6.0]	2.06 [0.88, 3.62]
50	-1.5	0 [0,0]	8.46 [5.57, 12.06]	63.24 [11.75, 216.11]
	-1	0 [0,0]	5.51 [3.45, 8.49]	17.26 [3.50, 67.67]
	-0.5	0 [0, 1.57]	2.53 [1.36, 5.01]	1.87 [0.51, 8.29]
	-0.1	1.83 [0, 2.37]	2.27 [1.44, 4.09]	1.86 [0.51, 3.2]
	0	1.98 [0.09, 2.45]	2.27 [1.37, 4.62]	1.61 [0.05, 3.39]
100	-1.5	0 [0,0]	10.56 [7.11, 13.92]	208.76 [61.32, 442.7]
	-1	0 [0,0]	7.02 [4.93, 8.84]	45.69 [6.44, 149.18]
	-0.5	0 [0, 1.43]	3.34 [1.61, 4.62]	3.67 [0.63, 15.55]
	-0.1	1.60 [0, 2.12]	2.04 [0.99, 2.45]	1.95 [0.61, 4.36]
	0	1.83 [0, 2.11]	2.13 [0.98, 4.41]	1.52 [0, 4.77]
150	-1.5	0 [0,0]	11.77 [8.74, 14.23]	392.29 [177.79, 835.42]
	-1	0 [0,0]	7.63 [5.80, 10.14]	80.58 [27.51, 232.06]
	-0.5	0 [0, 1.0]	3.50 [2.35, 6.11]	5.71 [0.42, 29.24]
	-0.1	1.45 [0, 2.17]	1.83 [0.81, 2.61]	1.6 [0.19, 6.49]
	0	1.81 [0, 2.18]	2.08 [1.02, 4.45]	1.67 [0, 5.98]

618

619 *Supplementary Figure 1.* As tree size and/or the degree of competition (*S*) increases, model

620 selection becomes more reliable. Comparison of Akaike weights (median & 90% CIs) for NH,

621 BM, OU, and EB models when simulated under various levels of competition (*S* = -1.5, -1, -0.5,

622 -0.1, and 0) for trees with 20, 50, 100, and 150 tips.

623

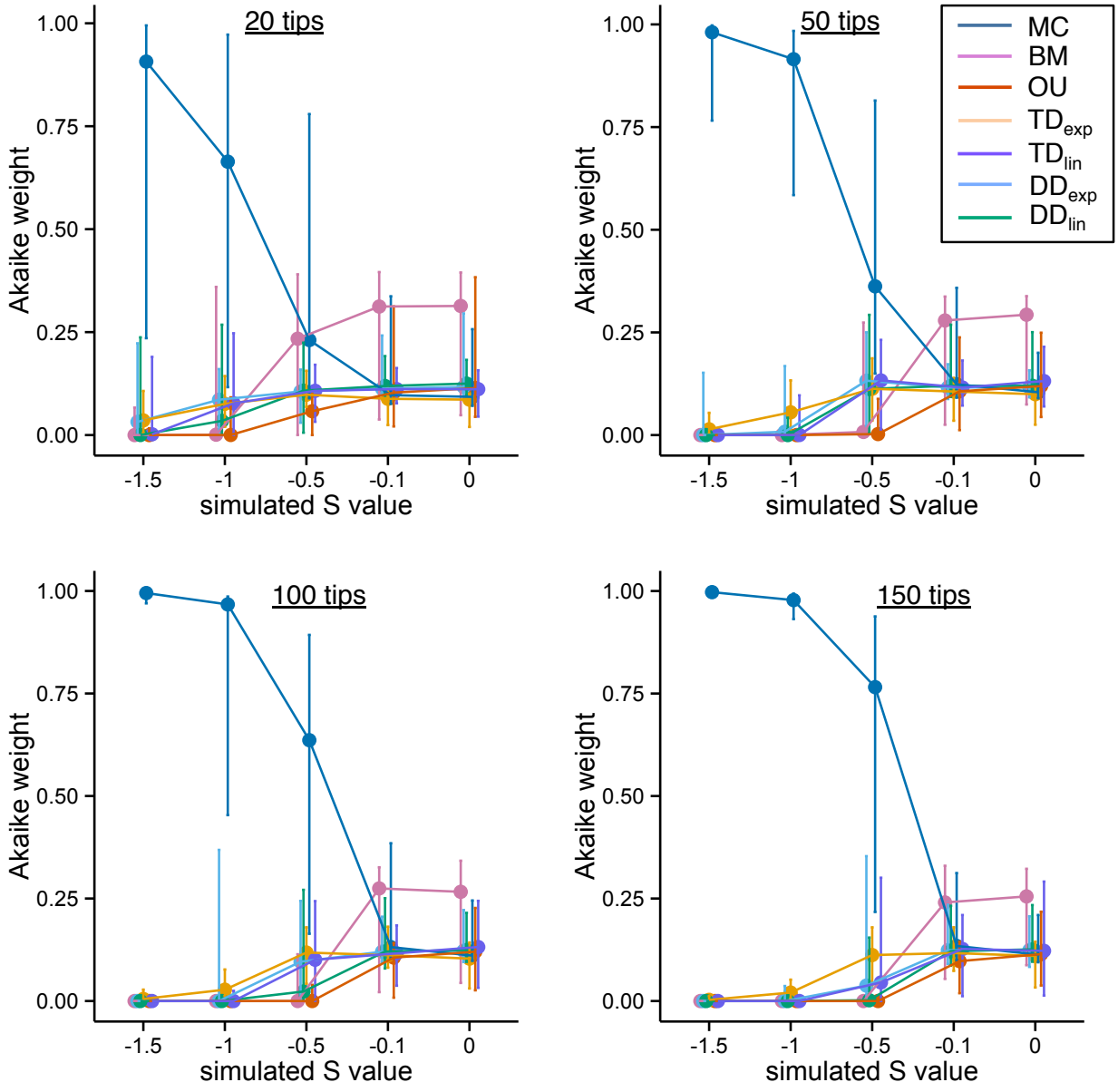

624
625
626

627 *Supplementary Figure 2.* Maximum likelihood estimates of ACDC rate parameters (i.e., TDexp
628 where rate parameters can take both positive and negative values) fit to data generated under the
629 matching competition model. As the level of competition increases (i.e., as *S* becomes
630 increasingly negative), the estimated rate parameter of the ACDC model becomes increasingly
631 negative.
632

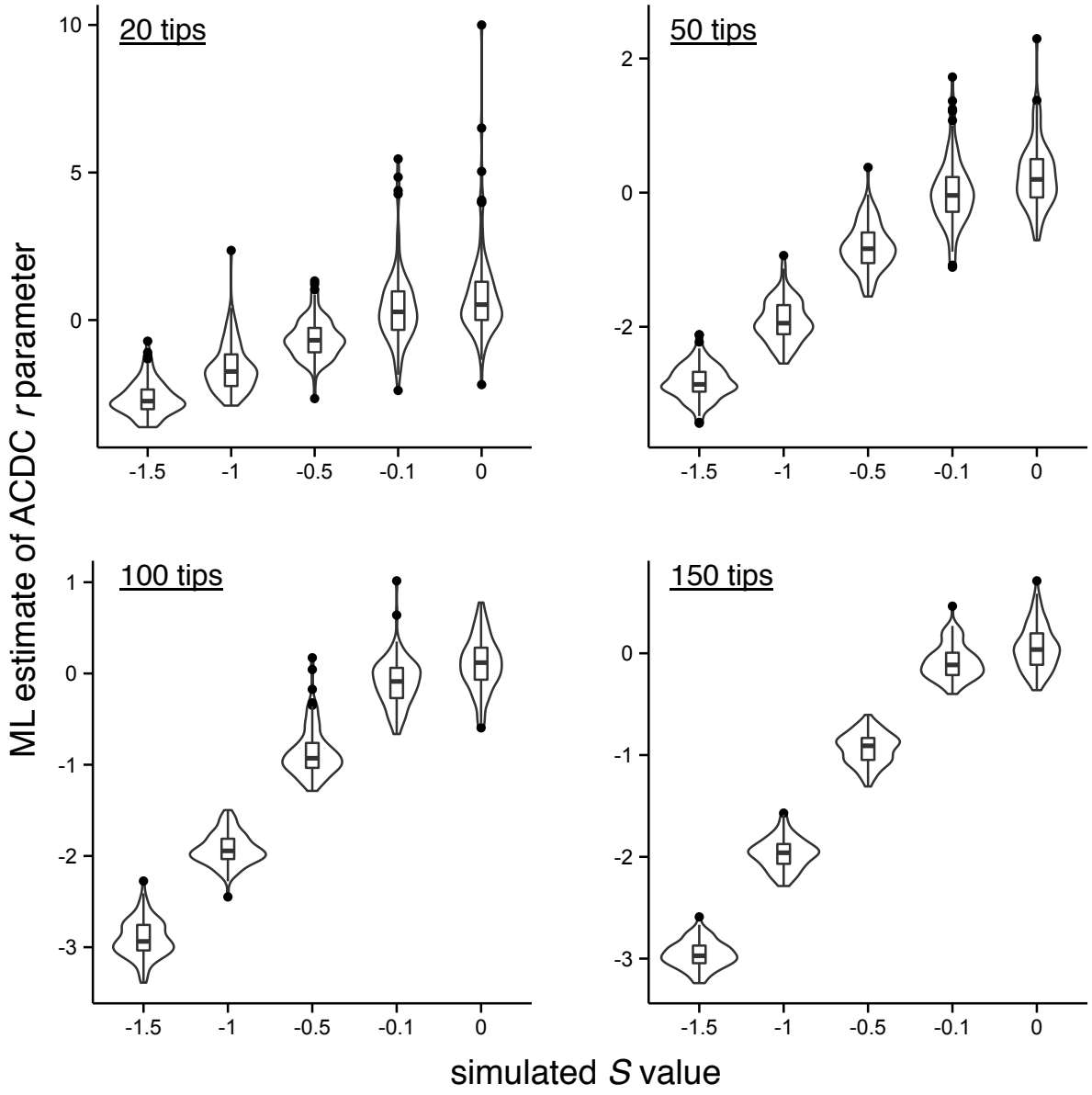

633

Supplementary Figure 3. Simulation results showing the effect of varying the extinction fraction on estimation of the *S* parameter for the matching competition model. Red horizontal lines indicate the simulated *S* values, and numbers above sets of simulations indicate the sample size of included simulations under those scenarios (see main text for more details).

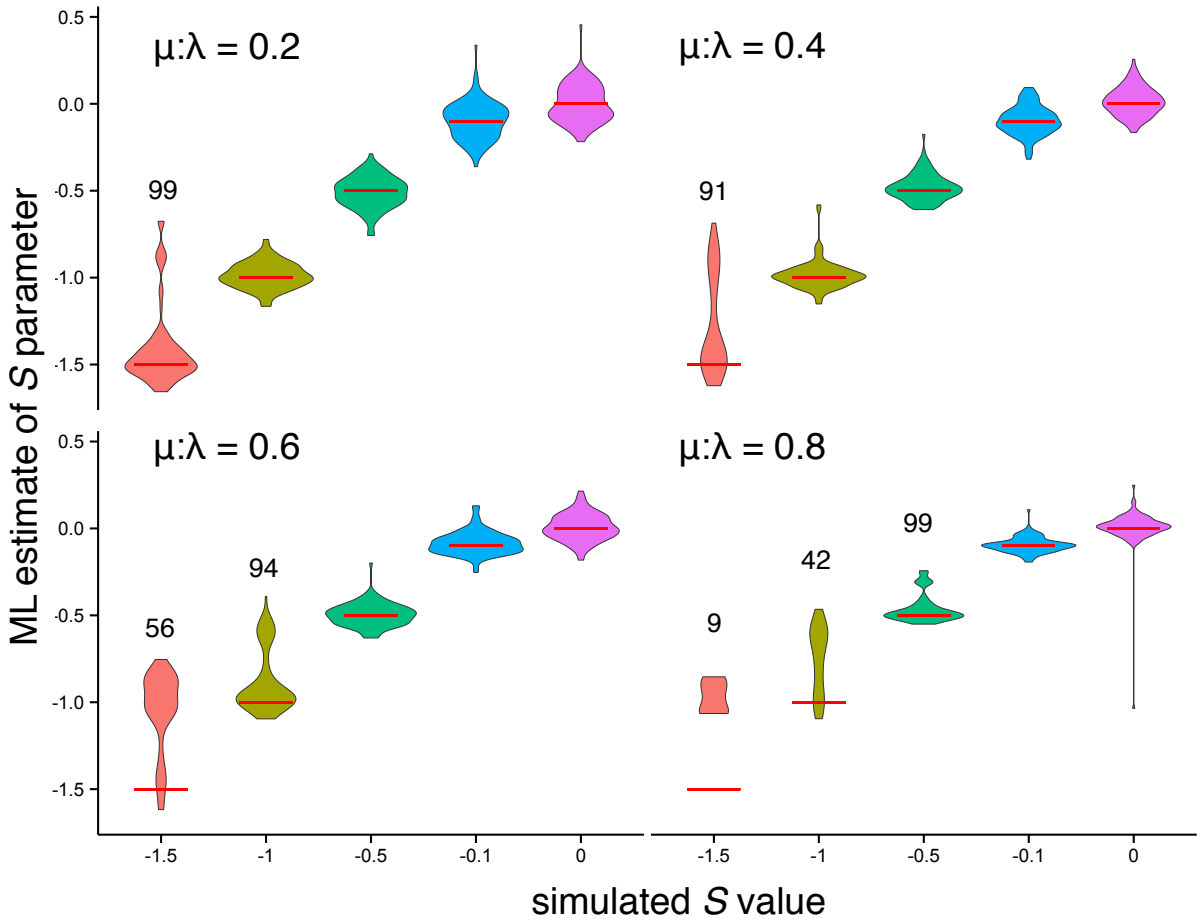

Supplementary Figure 4. Simulation results showing the effect of varying the extinction fraction on estimation of the σ^2 parameter for the matching competition model. Red horizontal lines indicate the simulated σ^2 value (0.05), the numbers below sets of simulations indicate the sample size of included simulations under those scenarios (see main text for more details), and the number in parentheses indicate sample size after σ^2 values > 0.25 re removed.

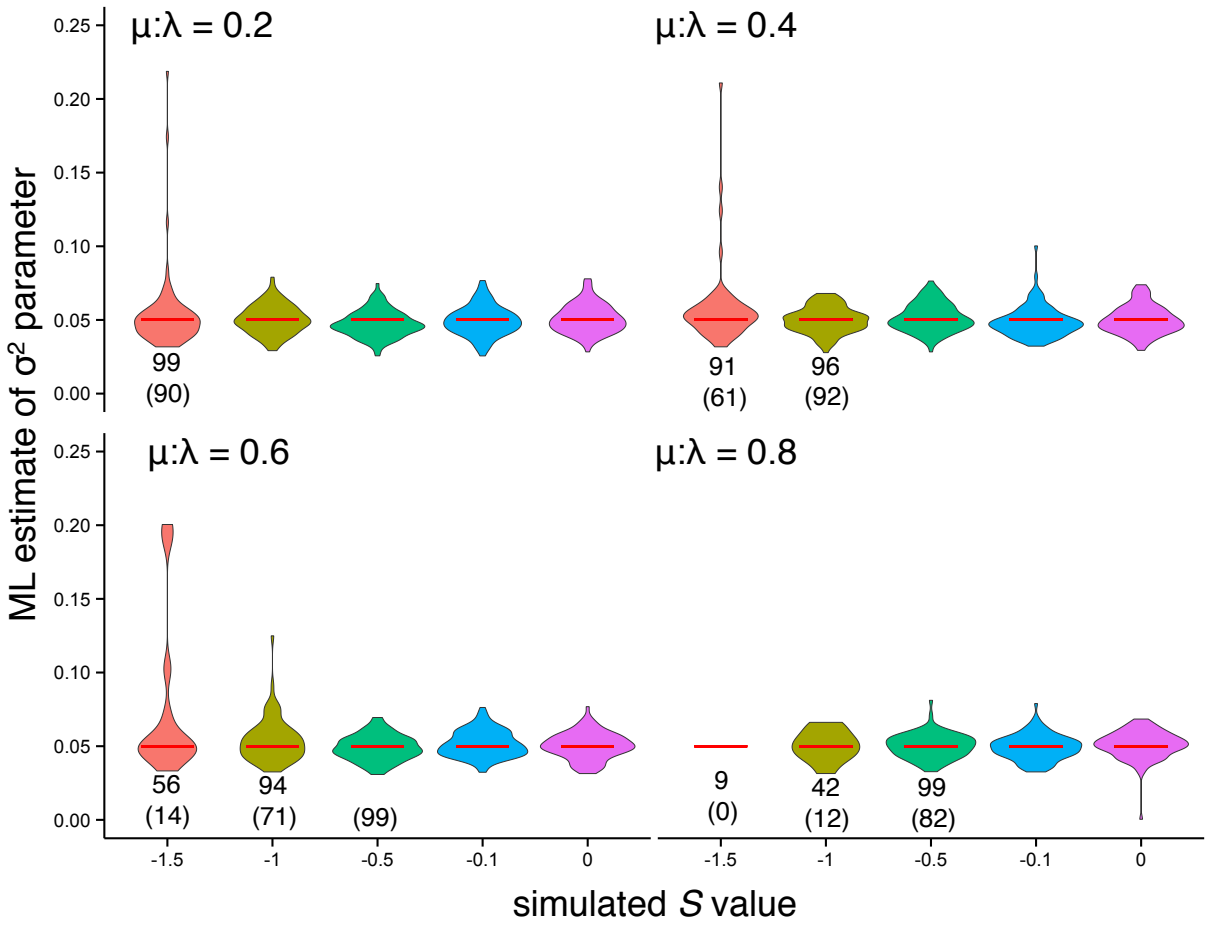

Supplementary Figure 5. Simulation results showing the effect of varying the extinction fraction on slope (top) and σ^2 (bottom) parameters for the exponential diversity-dependent model. Increasing extinction levels result in increasingly underestimated slope values and σ^2 parameters. Red horizontal lines indicate the simulated parameter values.

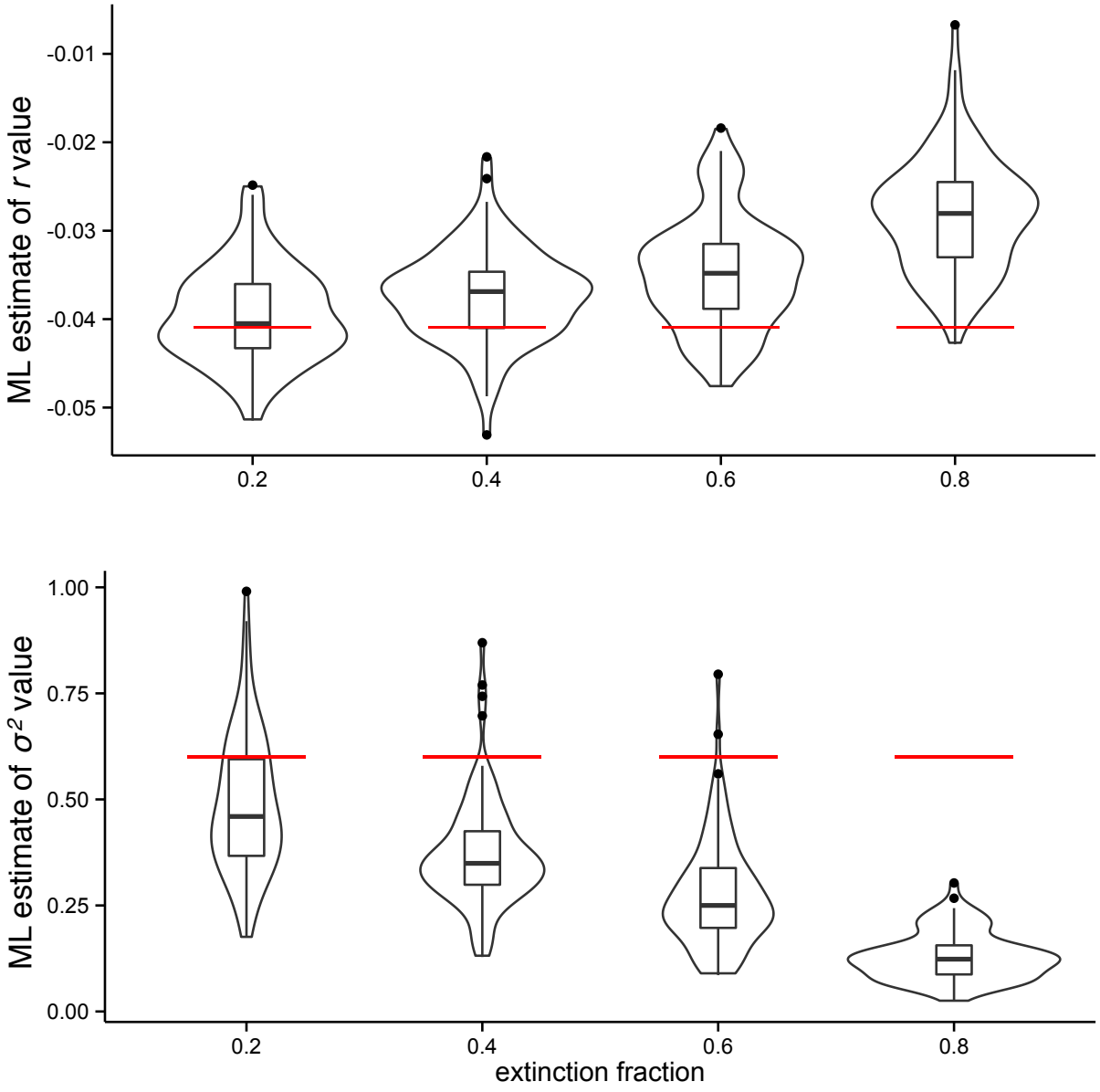
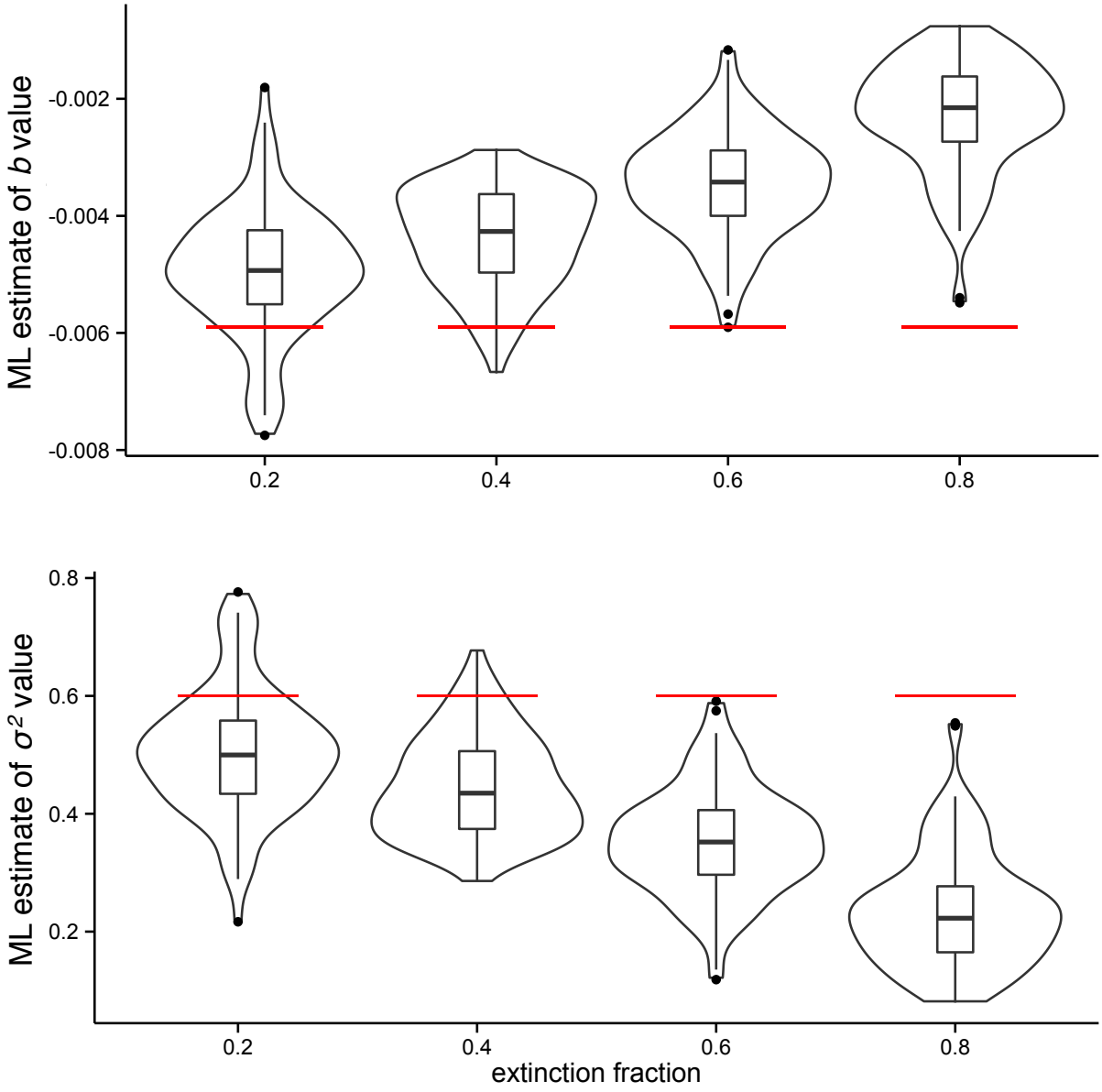
Supplementary Figure 6. Simulation results showing the effect of varying the extinction fraction on slope (top) and sigma-squared (bottom) parameters for the linear diversity-dependent model. Increasing extinction levels result in increasingly underestimated slope values and σ^2 parameters. Red horizontal lines indicate the simulated parameter values.